©2016 Published in 4th International Symposium on Innovative Technologies in Engineering and Science 3-5 November 2016 (ISITES2016 Alanya/Antalya - Turkey)

Numerical Investigation of Multi Square Jet Impingement for a Semi-Confined Channel

[1]*Perihan OCAL and [2]Nevin CELIK
*[1]Faculty of Engineering, Departman of Mechanical Engineering Bingol Univercity, Turkey
[2]Faculty of Engineering, Department of Mechanical Engineering Firat University, Turkey

Abstract

In this paper array of square jets from an orifice plate impinging to a target plate is taken into consideration. Jet density is represented with dimensionless jet-to-jet pitches (X_n/d for spanwise, Y_n/d for streamwise). X_n/d and Y_n/d are assumed to be equal and vary from 2 to 4. Distance between orifice plate and target plate is represented by dimensionless distance Z_n/d, which is changed from 2 to 4. The Reynolds number is taken as 5000, 10000 and 15000. Numerical results are discussed for different Reynolds numbers, jet-to-jet pitches (X_n/d, Y_n/d), and jet-to-target plate distances (Z_n/d). Finally it is found that, decreasing the jet-to-jet pitches results in a single channel flow characterization. Similarly decreasing the jet-to-target plate distances causes same effect on impingement.

***Keywords*— square jet, circler jet, numerical analysis, impingement, cooling**

1. Introduction

The impingement of an issuing jet onto a solid surface remarkably enhances local heat transfer rates during heating, cooling, or drying of the surfaces. Such a flow can easily be obtained with relatively low-cost and is used in a wide variety of engineering applications and industrial processes. The best examples are cooling / heating of hot / cold metal plates, drying of papers, textiles and foodstuffs, cooling of turbine blades and electronic components, and the de-icing of aircraft wings [1].

There are numerous investigations on the heat transfer and flow characteristics of an impinging jet in literature. Those researches are mostly related to the effects of design parameters on the impingement characters; i.e; jet types (circular or slot, single or multiply etc.) the nozzle shapes, jet exit velocity, jet-to-target surface distance etc. Since a jet array is considered in present research, the attention should be paid on that side. A considerable amount of research relating to the multiple-jet impingement heat transfer is performed [2]. Yong et al [3] experimentally investigated the effects of jet-to-jet pitch ratios in both streamwise and spanwise directions, jet-to-target spacing ratio and jet array arrangement (inline and staggered) on heat transfer. Vinze et al [4] experimentally investigated the influence of jet temperature and nozzle shape on the heat transfer distribution between a smooth plate and impinging air jets. Finally they marked that the affect of jet temperature on heat transfer is found marginal and axis swiching is observed for noncircular jets. Reodicar et al [5] experimently investigated influence of the orifice shape on the local heat transfer distribution and axis swiching by compressible jets impinging on flat surface. Their result show that the stagnation point Nusselt number is higher than other shapes(square, trianguler, elliptical) while

*Corresponding author: Address: Faculty of Engineering, Department of Mechanical Engineering Bingol University, Bingol,TURKEY. E-mail address: pocal@bingol.edu.tr , Phone: +905078328786

that for the elliptical orifice is minimum. Square, trianguler, and elliptical orifice respectively ondergoesa 45°, 180°, and 90° axis swiching. In the another study on different nozzle geometry Trinh et al [6] the effect of nozzle geometry on local convective heat transfer to unconfined impinging air jets investigated. In this study round orifice and cross-shaped geometry take in to consideration for $23000 \leq Re \leq 45000$ Reynold number. According to their results, round orifice on the hemisphere causes higher heat transfer rate than the cross-shaped orifice.

Behbahani and Goldstein [7] used the liquid crystal technique to evaluate heat transfer for a staggered array of jets impinging on a flat surface and gave qualitative results relatively to the jet-to-target plate distance. Caliskan et al [8] performed both numerical and experimental researches in order to find out the effect of jet geometry on the flow and the heat transfer characteristics is for elliptic and rectangular impinging jet arrays. It is finally marked that heat transfer for the elliptic jets in the impingement regions is higher than that for a circular jet. Furthermore the best heat transfer performance is obtained with the elliptic jet arrangements.

Pertrand et al. [9] investigated a better understanding of the mean flow characteristics and heat transfer of jet array with cross-flow, using different jet orifice geometries, circular and cusped ellipse. Puneet et al. [10] investigated the effect of nozzle shape on local heat transfer distribution for circular, square and rectangular nozzle cross sections. Aldabbagh and Sezai [11] numerically investigated the flow and heat transfer characteristics of impinging laminar multiple square. The results showed that the flow structure of multiple square jets impinging on a heated plate is strongly affected by the jet-to-plate distance. On the other hand, the magnitude of the local maximum Nusselt number at the stagnation point is not affected by jet-to-jet spacing. Mikhail et al. [12] numerically studied the flow and heat transfer characteristics of jets issuing from a row of slots and impinging normally on a flat plate. Their results show that the average Nusselt number increases as the nozzle-to-plate spacing decreases. Lee et al.[13] investigated heat transfer with fully developed slot jets impinging on confined concave and convex surfaces. The results show that peak stagnation point Nusselt numbers occur at around nozzul-to-surface distance between 5-7 for the convex surface, on the contrary stagnation point Nusselt numbers for the concave surface tend to gradually decrease as the nozzle-to –surface distances increases. Also the stagnation point Nusselt numbers for the concave surface are higer than those for the convex surface at all Re's and nozzle-to – surface distances tested.

In present study the effects of jet-to-jet pitch ratios in both streamwise and spanwise directions and jet-to-target spacing ratio on the jet impingement heat transfer behaviors are numerically investigated under the jet Reynolds number ranged from 5000 to 15000. It is especially aimed to analyze the dense-array jet impingement phenomena inside a semi-confined channel with one-directional spent air outflow where the jet-induced crossflow is more serious.

2. Numerical Study

2.1. Physical Model and Boundaries

The physical model is represented in Fig 1. As it is seen in figure, the model is composed of a target plate, orifice plate, front plate and two side plates. The streamwise width (y-direction) is 40 mm and the spanwise length (x-direction) is 20 mm. The thermal conductivity of orifice plate is very low to

minimize the heat transfer. Multiple rectangle holes, arranged in inline array, are used to generate the impinging jets. The hydraulic diameter of the jet (d) is equal to 2 mm. The first row of array jets is positioned at 3d downstream from the closed end of the test section, as sketched in Fig 1. In the present study, the streamwise jet-to-jet pitch ratio (Y_n/d) is designed equal to the spanwise jet-to-jet pitch ratio (X_n/d) for all the cases. The number of jet rows varied according to the streamwise jet-to-jet pitch, (9, 6 and 5), corresponding to the streamwise jet-to-jet pitch ratio of 2, 3 and 4. The impingement target's width (y-direction) is 40 mm and the length is 20 mm.

The impingement distance or the jet-to-target spacing between the orifice plate and the target plate (Z_n/d) is varied as 2, 3 and 4. Similarly, the distance between jets at y-direction namely; the streamwise jet-to-jet pitch ratio (Y_n/d) varied as 2, 3 and 4, while the spanwise jet-to-jet pitch ratio (X_n/d) varied as same.

Figure 2 refers to the fluid domain with the details of boundary conditions. The whole solution domain consists of three side walls, one outlet, jet inlets and one target wall. At each of the jets' inlets, the velocity is shown via dimensionless Reynolds number, which varied as 5000, 10000 and 15000.

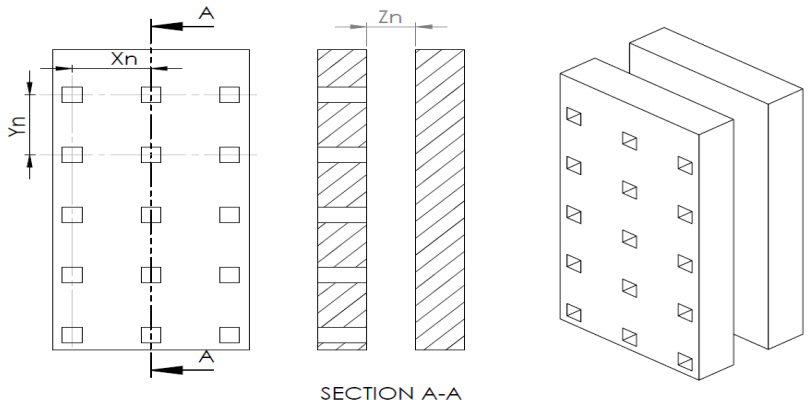

Figure 1. Physical model

The used jet flow is air and the properties of air are specified for static temperature at 25 °C. At the inlet of the solution domain, the temperature is assumed to be uniform and equal to the ambient temperature (25°C). The outlet of solution domain is taken as under the condition of atmospheric pressure. Simulation is performed for thermal energy, and target wall is heated at constant heat flux; 9000 W/m^2. The orifice plate and the jet walls are considered as adiabatic smooth walls. The study is performed by using CFX 14.5. Mesh independence is provided there by taking three edges of element length sizes; 0.2, 0.25 and 0.3 mm. Accuracy is ensured by requiring that all residuals reduced to 10^{-6} at the end of the computer run. %0.5 mesh accuracy is obtained with an overall node number; 5 million.

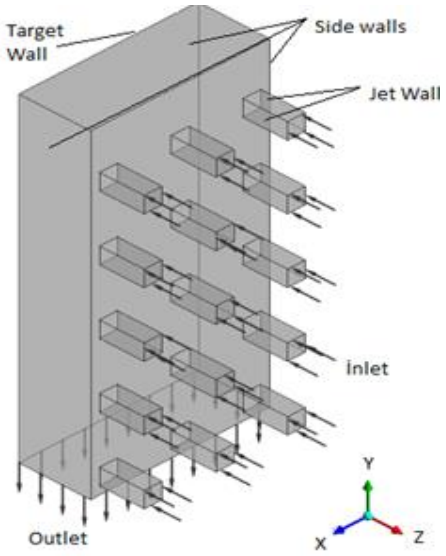

Figure 2. Solution domain

2.2. Mathematical Model and Governing Equations

The conducted numerical simulation is based on RANS form of momentum and mass conservation equations. The well-known *k-ε* model is considered as the turbulence model. In the *k-ε* model, the first variable determines the energy in the turbulence and is called as turbulent kinetic energy (*k*). The second transported variable is the turbulent dissipation (*ε*) which determines the rate of dissipation of the turbulent kinetic energy [14].

The RANS equations used here are stated in Cartesian tensor form for conciseness in equation (1).

$$\rho\left(u_i\frac{\partial u_j}{\partial x_i}\right) = -\frac{\partial p}{\partial x_i} + \frac{\partial}{\partial x_i}\left((\mu+\mu_t)\frac{\partial u_j}{\partial x_i}\right) \quad \text{j = 1, 2, 3} \tag{1}$$

In this equation the quantity μ_t is readily identified as the turbulent viscosity. The conservation of mass equation represented by equation (2) for incompressible flow.

$$\frac{\partial u_i}{\partial x_i} = 0 \tag{2}$$

The turbulent kinetic energy *k* and the dissipation *ε* are represented by (3) and (4) equations respectively,

$$\frac{\partial \rho k}{\partial t} + \frac{\partial \rho k u_i}{\partial x_i} = \frac{\partial}{\partial x_i}\left(\frac{\mu_t}{\sigma_k},\frac{\partial k}{\partial x_i}\right) + 2\mu_t E_{ij}E_{ij} - \rho\varepsilon \tag{3}$$

$$\frac{\partial \rho \varepsilon}{\partial t} + \frac{\partial \rho \varepsilon u_i}{\partial x_i} = \frac{\partial}{\partial x_i}\left(\frac{\mu_t}{\sigma_\varepsilon}, \frac{\partial \varepsilon}{\partial x_j}\right) + c_{1\varepsilon}\frac{\varepsilon}{k} 2\mu_t E_{ij} E_{ij} - C_{2\varepsilon}\rho\frac{\varepsilon^2}{k} \quad (4)$$

where u_i, E_{ij} and μ_t represent the velocity component in corresponding direction, the component of rate of deformation and the turbulent viscosity, respectively. The viscosity also characterized by equation (5)

$$\mu_t = \rho C_\mu \varepsilon^2 \quad (5)$$

The equations also consist of some adjustable constants σ_k, σ_ε, $C_{\varepsilon 1}$, $C_{\varepsilon 2}$. The values of these constants have been arrived at by numerous iterations of data fitting for a wide range of turbulent flows; C_μ=0.09, σ_k=1.0, σ_ε=1.30, $C_{\varepsilon 1}$=1.44 and $C_{\varepsilon 2}$=1.92.

If a turbulent Prandtl number is defined as equation (6), then the energy equation can be represented by equation (7)

$$\mathrm{Pr}_t = \frac{C_p \mu_t}{k_t} = 0.9 \quad (6)$$

$$\rho c_p\left(u_i \frac{\partial T}{\partial x_i}\right) = \frac{\partial}{\partial x_i}\left((k + k_t)\frac{\partial T}{\partial x_i}\right) \quad (7)$$

In this equation, k is the molecular thermal conductivity (a fluid property), and k_t is the turbulent thermal conductivity respectively.

3. Results and Discussions

Figures 3 and 4 show the local heat transfer coefficient contour corresponding to different jet-to-jet pitches a) X_n/d = 2, b) X_n/d = 3, c) X_n/d = 4 respectively on the impinging target for *Re* = 15000. It is seen from the contours that, the single jet impingement feature is rarely observed for the lowest jet-to-jet pitch ratio (X_n/d = 2) whilst it is strongly observed for the highest jet-to-jet pitch ratio (X_n/d = 4). Due to the strong adjacent jet interference, the flow inside array jets impingement dominated region is more likely a channel flow, even at large jet-to-target spacing ratio of 4 [3].

Figure 5 and Figure 6 respectively exhibit the averaged *Nu* numbers along the streamwise direction under condition of *Re* = 15000, for Z_n/d = 2 and 4. The heat transfer in the case of impingement especially for different X_n/d is significant in these figures. For X_n/d = 4, the averaged *Nu* number corresponding to the impinging jet stagnation is obviously higher and weakly affected by the jet-induced crossflow inside the confined channel.

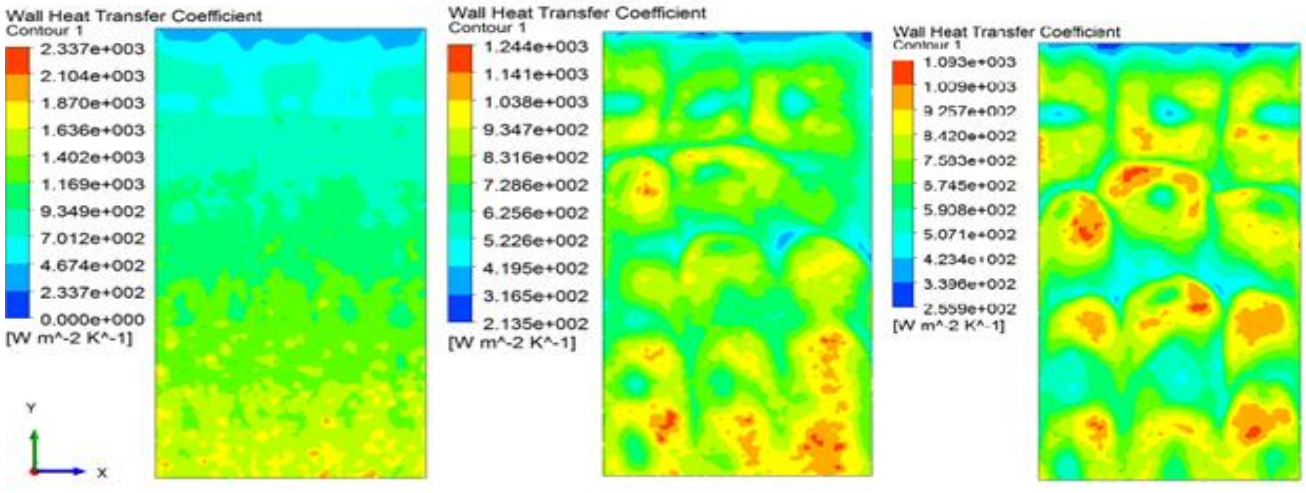

a) b) c)

Figure 3. Local heat transfer coefficient for *Re* = 15000, Z_n/d = 2, a)X_n/d =2, b)X_n/d =3 , c) X_n/d = 4

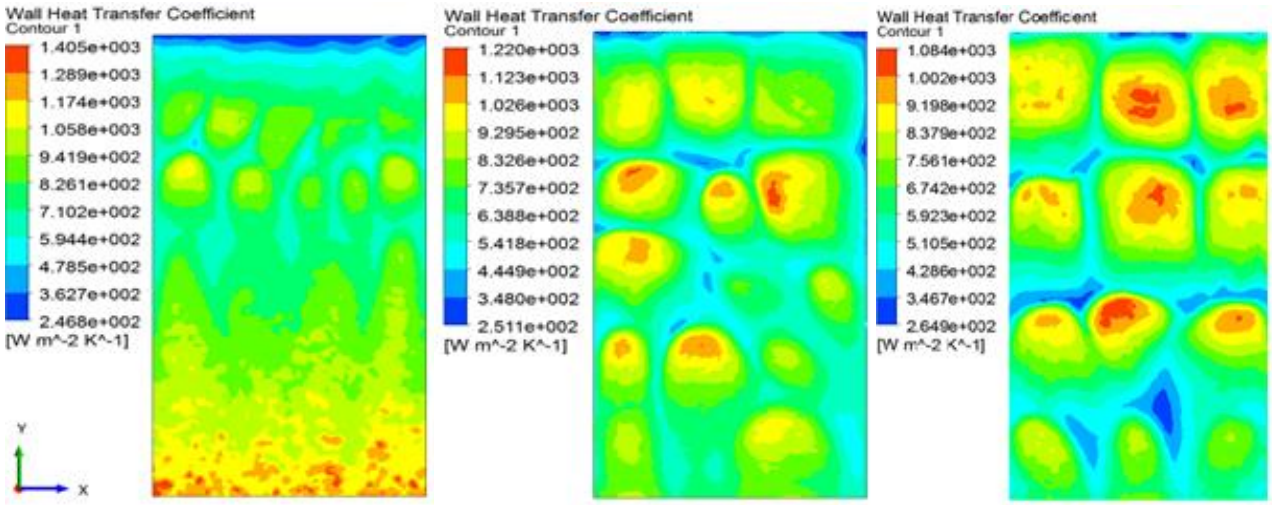

a) b) c)

Figure 4. Local heat transfer coefficient for *Re* = 15000, Z_n/d = 4, a) X_n/d = 2, b) X_n/d = 3, c)X_n/d =4

This result also can be seen from Figures 7 and 8, which represent local heat transfer coefficient contour plots of various jet-to-target spacing ratio, which represented by a) Z_n/d =2, b) Z_n/d = 3 and c) Z_n/d = 4 respectively (for *Re* = 15000, X_n/d = 2 and 4). For densest jet array (X_n/d = 2) flow characteristic is like a channel flow, there is no stagnation point effect; but for rare jet to jet distances (X_n/d = 4) stagnation point effect is dominant.

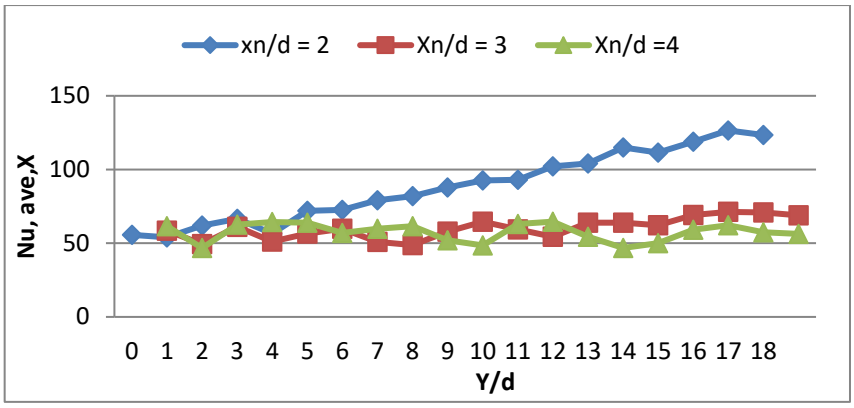

Figure 5. Averaged *Nu* number along the streamwise direction for *Re* = 15000, Z_n/d = 2

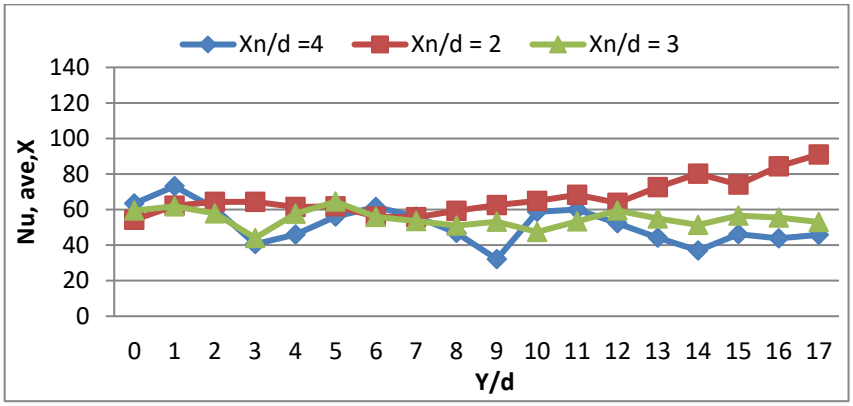

Figure 6. Averaged *Nu* number along the streamwise direction for *Re* = 15000, Z_n/d =4

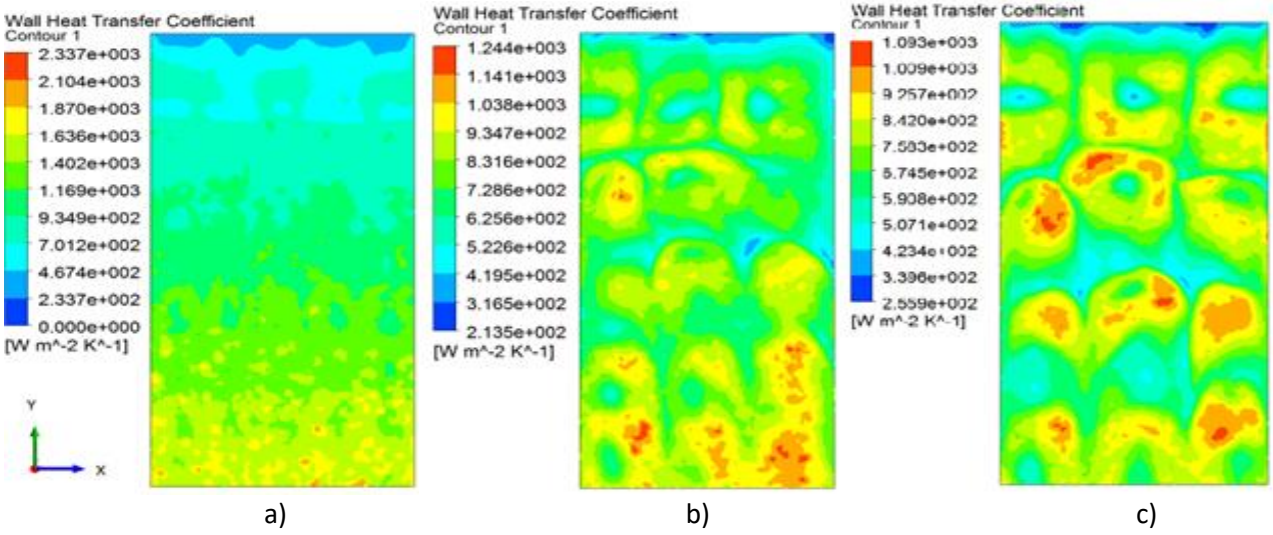

Figure 7. Local heat transfer coefficient for Re = 15000, X_n/d = 2 a) Z_n/d =2, b) Z_n/d = 3, c) Z_n/d = 4

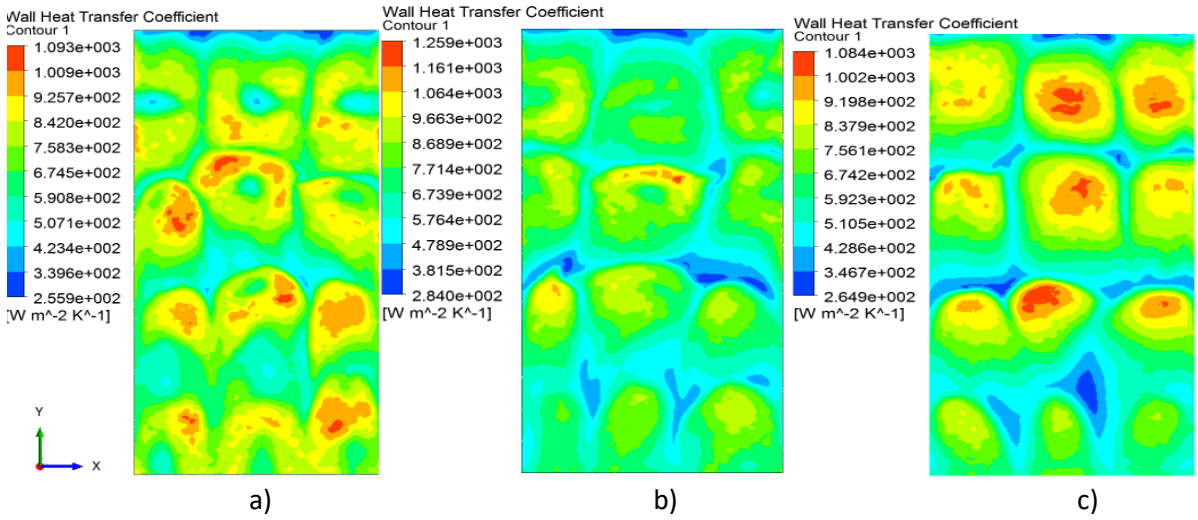

Figure 8. Local heat transfer coefficient for Re = 15000 $X_n/d = 4$ a) $Z_n/d = 2$, b) $Z_n/d = 3$, c) $Z_n/d = 4$

The streamwise average *Nu* numbers corresponding to different jet-to-jet pitches under jet-to-target spacing ratio of 2 and 4 are presented in Fig. 9 and Fig. 10 for *Re* = 15000 and jet-to-jet pitch X_n/d = 2. As the convective heat transfer by the channel flow in the rear rows of jet impingement is augmented due to the strong jet-induced crossflow, the streamwise average Nusselt number is increased rapidly along the streamwise direction under the densest-array jet impingement. It is clear that the 'channel-like flow' effect is more significant in the confined multiple jets impingement when the target plate is very close to the jet exit.

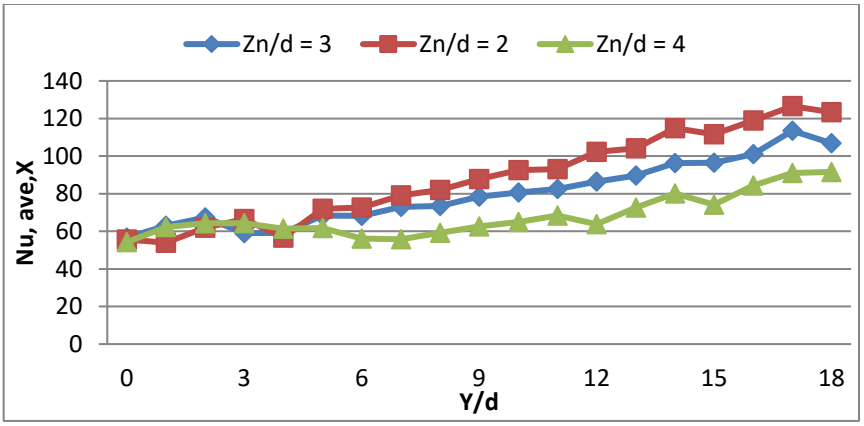

Figure 9. Averaged *Nu* number along the streamwise direction, of varios Z_n/d, *Re*=15000 $X_n/d = 2$

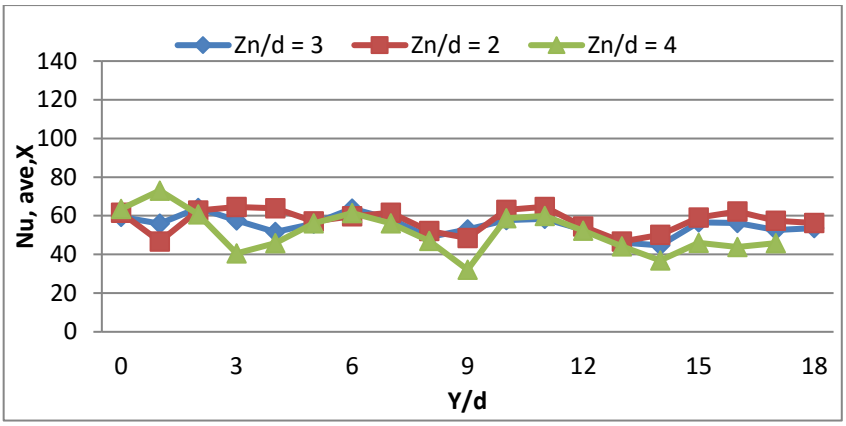

Figure 10. Averaged *Nu* number along the streamwise direction, of various Z_n/d, for *Re*=15000, $X_n/d = 4$

Figure 11 plots the Nusselt number versus streamwise direction for various *Re* numbers at a constant value of jet-to-jet pitch and jet-to-target plate distance. It is evident from the figures that increasing Re number results in increasing heat transfer as already expected.

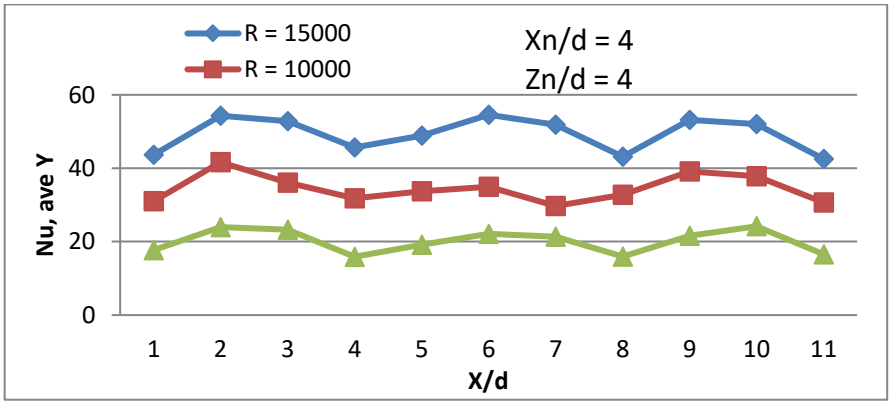

Figure 11. Averaged *Nu* number respect to various *Re* numbers for X_n/d=4, Y_n/d=4

Conclusions

The effects of the jet-to-jet pitch ratio (X_n/d; 2 to 4) and jet-to-target spacing ratio (Z_n/d; 2 to 4) on the jet impingement heat transfer for jet Reynolds number ranged from 5000 to 15000 are numerically predicted by using CFX software. The attention is mostly paid to dense-array jet impingement behaviors. It was seen that because of the strong adjacent jet interference, the flow inside the impingement dominated region by the densest-array jet impingement ($X_n/d = Y_n/d = 2$) is more likely a channel flow.

The heat transfer performance for the jet-to-target spacing ratio of $Z_n/d = 2$ is confirmed to be superior to that of Z_n/d =3 or $Z_n/d = 4$ for the dense array of multiple jets, which is consistent to the previous founding for the sparse array of multiple jets.

There are numerous investigations on different cooling, heating and drying methods. Jet

impinging heat transfer take important places in such areas. This heat transfer method either have low cost or have easy applicability. So there are numerious research on jet impingement study and of course such works will be continues in the future. For this reason such that study would be referred by academic and industrial areas in heating, cooling and drying. Also it can be referred by studies which included square nozzle shape for heat transfer coefficient or Nusselt number.

References

[1] H. Eren, B. Yesilata, and N.Celik, "Nonlinear flow and heat transfer dynamics of impinging jets onto slightly-curved surfaces" Applied Thermal Engineering, vol. 27, pp.14-15, 2007.

[2] B. Weigand, S. Spring, "Multiple jet impingement – a review", Heat Transfer Res., vol.42, pp.101–142, 2011.

[3] S. Yong, Z. Jing-Zhou, X.Gong-nan, ''Convective heat transfer for multiple rows of impinging air jets with small jet-to-jet spacing in a semi-confined channel", Int. J. of Heat and Mass Trans., vol. 86 832–pp. 842, 2015.

[4] R. Vinze, S.Chandel, L.Limaye, S.V. Prabhu ,''Influence of jet temperature and nozzle shape on the heat transfer distribution between smooth plate and impinging air jets'', Int. J. Therm. Sci., vol. 99, pp. 136–151, 2016.

[5] S.A.Reodicar, H. C. Meena, R.Vinze, S.V. Prabhu '' Influence of the orifice shape on the local heat transfer distribution and axis swiching by compressible jets impinging on flat surface'', Int. J. Therm. Sci., vol. 104, pp. 208-224, 2016.

[6] X. T. Trinh, M. Fenot, E. Dorignac, '' effect of nozzle geometry on local convective heat transfer to unconfined impinging air jets'', Experimental Thermal And Fluid Science, vol. 70, pp. 1–16,

[7] A.I. Behbahani and R.J. Goldstein, "Local heat transfer to staggered arrays of impinging circular air jets", J. Eng. Power, vol. 105, pp. 354–360. 1983.

[8] S. Caliskan, S.Baskaya, T. Calisir, "Experimental and numerical investigation of geometry effects on multiple impinging air jets", Int.J. of Heat and Mass Trans., vol. 75, pp. 685–703, 2014.

[9] P.E. Pertrand, A.J. Liburdy, K. Kanokjaruvijit, "Flow characteristics and heat transfer performances of a semi-confined impinging array of jets, effect of nozzle geometry", Int. J. Heat Mass Transfer, vol. 48 pp.691–701, 2005.

[10] G. Puneet, K. Vadiraj, S.V. Prabhu, "Influence of the shape of the nozzle on local heat transfer distribution between smooth flat surface and impinging air jet", Int. J. Therm. Sci., vol. 48, pp. 602–617, 2009.

[11] L.B.Y. Aldabbagh, I. Sezai, "Numerical simulation of three-dimensional laminar multiple impinging square jets", Int. J. of Heat and Fluid Flow, vol.23, pp. 509–518, 2002.

[12] S. Mikhail, S.M. Morcos, M.M.M.Abou-Ellail, W.S. Ghaiy, "Numerical prediction of flow field and heat transfer from a row of laminar slot jets impinging on a flat plate", Proc. 7th Int. Heat Transfer Conf. vol. 3, pp.377–382, 1982.

[13] D.H. Lee, S. J. Kim, Y. H. Kim, H. J. Park, ''Heat transfer with fully developed slot jets impinging on confined concave and convex surfaces'', Int. J. Heat Mass Transfer, vol. 88 pp.218–223, 2015.

[14] B.E. Launder, and D. B. Spalding, "The numerical computation of turbulent flows", Computer Methods in Applied Mech. and Eng. Vol. 3, pp. 269-289, 1974.